



ELSEVIER

Available online at www.sciencedirect.com

SCIENCE @ DIRECT®

Journal of Contaminant Hydrology 62–63 (2003) 319–336

JOURNAL OF

Contaminant
Hydrology

www.elsevier.com/locate/jconhyd

A geostatistical modeling study of the effect of heterogeneity on radionuclide transport in the unsaturated zone, Yucca Mountain

Hari S. Viswanathan*, Bruce A. Robinson,
Carl W. Gable, James W. Carey

Earth and Environmental Sciences Division, Los Alamos National Laboratory, Los Alamos, NM 87545, USA

Abstract

Retardation of certain radionuclides due to sorption to zeolitic minerals is considered one of the major barriers to contaminant transport in the unsaturated zone of Yucca Mountain. However, zeolitically altered areas are lower in permeability than unaltered regions, which raises the possibility that contaminants might bypass the sorptive zeolites. The relationship between hydrologic and chemical properties must be understood to predict the transport of radionuclides through zeolitically altered areas. In this study, we incorporate mineralogical information into an unsaturated zone transport model using geostatistical techniques to correlate zeolitic abundance to hydrologic and chemical properties. Geostatistical methods are used to develop variograms, kriging maps, and conditional simulations of zeolitic abundance. We then investigate, using flow and transport modeling on a heterogeneous field, the relationship between percent zeolitic alteration, permeability changes due to alteration, sorption due to alteration, and their overall effect on radionuclide transport. We compare these geostatistical simulations to a simplified threshold method in which each spatial location in the model is assigned either zeolitic or vitric properties based on the zeolitic abundance at that location. A key conclusion is that retardation due to sorption predicted by using the continuous distribution is larger than the retardation predicted by the threshold method. The reason for larger retardation when using the continuous distribution is a small but significant sorption at locations with low zeolitic abundance. If, for practical reasons, models with homogeneous properties within each layer are used, we recommend setting nonzero K_d s in the vitric tuffs to mimic the more rigorous continuous distribution simulations. Regions with high zeolitic abundance may not be as effective in

* Corresponding author. Tel.: +1-505-665-6737.

E-mail address: viswana@lanl.gov (H.S. Viswanathan).

retarding radionuclides such as Neptunium since these rocks are lower in permeability and contaminants can only enter these regions through molecular diffusion.

Published by Elsevier Science B.V.

Keywords: Unsaturated flow and transport; Numerical modeling; Heterogeneous media; Zeolitic tuffs

1. Introduction

Natural spatial variability in hydrologic and chemical properties can play an important role in the transport of contaminants in groundwater. Stochastic techniques to study the effects of small-scale variability are common in the groundwater literature (Gelhar, 1993). Tompson and Jackson (1996) review the correlations that have been used to relate hydrologic and transport properties in heterogeneous systems. For example, many investigators have observed that the sorption distribution coefficient (K_d) is inversely correlated to the natural log of permeability in support of theoretical and computational studies designed to evaluate the effect of spatially variable retardation on plume migration. Reduction in sorption due to physical and chemical heterogeneity has also been described by Tompson et al. (1996) and Smith et al. (1996). They suggest that for the saturated flow system they studied, significant contaminant transport will occur in zones of minimal reactivity since permeability and reactivity are inversely correlated in the materials they investigated. In the unsaturated zone, Birkholzer and Tsang (1997) show that solute channeling can be prevalent in strongly heterogeneous and variably saturated porous media.

Zeolites sorb and retard many of the radionuclides that will be present in the waste inventory. However, zeolitically altered areas of the tuff that make up the stratigraphy of Yucca Mountain are lower in permeability than the unaltered vitric areas. Site-scale models of Yucca Mountain typically rely on averaging techniques in order to model the large scales that are of interest in the flow and transport calculations. For zeolites, the usual assumption made in the previous work has been to use a threshold cutoff for zeolitic abundance (Robinson et al., 1997; Bodvarsson et al., 1999), above which the medium is given properties of “zeolitic rock” and below which the medium is given properties of vitric tuff.

There are limitations to this approach that must be addressed. First, the choice of the threshold cutoff can dramatically affect the nature of the resulting zeolite distribution. Low values of the parameter result in more continuous distributions of zeolitic rock, as greater portions of the rock are given the attribute “zeolite.” In contrast, higher cutoff values result in a more patchy distribution of zeolites. If in the hydrologic model developed from this distribution we assign other parameters with widely contrasting values such as permeability, the model becomes very dependent on the threshold cutoff chosen. Therefore, the threshold cutoff chosen can strongly affect the scale of the zeolite distributions with lower cutoff values leading to larger correlation lengths. In reality, there is a continuous distribution of percent zeolitic alteration that cannot be captured by a threshold model. To properly account for this heterogeneity, we must understand the relationship between zeolitic alteration, hydrologic properties (e.g. permeability) and chemical properties (K_d) and build numerical models that explicitly account for the variability. Since we are concerned with zeolite heterogeneity in the unsaturated zone, the large-scale hydro-

logic behavior of the rock under unsaturated conditions must be considered. Only after performing such an analysis would we understand the system well enough to support the use of more simplified homogeneous models.

In the present study, we examine how the heterogeneity of zeolitic minerals that lie in-between the potential repository at Yucca Mountain and the water table affects radionuclide transport. In this study, we examine the impact of small-scale variability in the zeolite distribution on the transport of ^{237}Np through the unsaturated zone. Because of its long half-life (2.14×10^6 years), relatively high solubility under oxidizing conditions, low dose limits, and predicted low sorption, performance assessment models have identified ^{237}Np as a radionuclide of concern for the proposed repository at Yucca Mountain (Andrews et al., 1995; DOE, 1998). We use conditional simulations of zeolitic abundance to determine whether small-scale heterogeneities will significantly affect the travel times of ^{237}Np through the unsaturated zone. Site data on zeolite abundance are used to condition the model, and laboratory scale measurements are reviewed to provide basis for the correlations between zeolite abundance and hydrologic and transport properties. These results are then imported into a two-dimensional, site-scale flow and transport model that resolves the behavior in detail. Because we present results of an analysis using a single flow and transport realization, a complete analysis of property variability and its influence on the uncertainty of the transport results is beyond the scope of this study. However, the basic processes and the influence of small-scale heterogeneity are uncovered by the model, thereby allowing us to assess the validity of more simplified modeling approaches.

2. Mineralogical data and modeling

2.1. Three-dimensional mineralogic model

A three-dimensional model of the distribution of mineralogy at Yucca Mountain was developed to allow calculations of hydrology and transport. A geostatistical approach was used in developing the model to provide: (1) insight into the variability of the data; (2) characterization of the uncertainty in the areas surrounding the data; (3) an unbiased best estimate of values in unsampled areas; and (4) simulated (stochastic) distributions of mineralogy based on the observed population statistics. This approach results in a fully populated stochastic site-scale numerical mineralogic model that can be used as a basis for transport calculations.

The mineralogic model was developed from quantitative X-ray diffraction of approximately 1000 core and cuttings samples taken at 21 drill holes in the Yucca Mountain region. Quantitative XRD provides an accurate and direct measurement of mineralogy (Chipera and Bish, 1995), and as practiced here yields an average mineral abundance that is most applicable to calculations involving matrix flow (fracture mineralogy at Yucca Mountain is distinct from matrix mineralogy).

The mineralogy at Yucca Mountain varies as a function of the degree of devitrification and alteration of the volcanic tuff layers. As a consequence, the mineral distribution is partly a function of stratigraphy. The software package Stratamodel (Landmark Graphics, 1995) was used to model the three-dimensional mineral distribution within a stratigraphic

framework. The stratigraphic model consists of 30 units based on the stratigraphy of Zelinski and Clayton (1996). The three-dimensional mineral distribution was calculated for each stratigraphic unit after assigning drill hole data to its proper stratigraphic unit. The model consists of two parts: an inverse-distance weighted model for the entire mineral data set (Carey et al., 1997) and a separate geostatistical (kriged) version of just the zeolite data (discussed in more detail below).

The modeled distribution of zeolites at Yucca Mountain is the sum of clinoptilolite + mordenite + erionite + stellerite + chabazite (clinoptilolite and mordenite are the most important species). The abundance of zeolite varies across the repository block, but the most significant deposits occur at depths greater than about 100 m above the water table. At these depths, zeolites are generally found in the altered vitric upper and lower portions of the volcanic tuff units, not in the devitrified centers. However, one of the key stratigraphic units below the proposed repository horizon, the Calico Hills Formation, does not have a devitrified center and contains volcanic glass, zeolites, or a mixture of both. The stratigraphic depth of significant zeolite occurrences increases towards the southwest part of the study region, but the available data indicate that there are zeolite-bearing zones everywhere between the proposed repository horizon and the water table.

The abundance of zeolites at Yucca Mountain shows a bimodal distribution divided between altered volcanic tuff with abundant zeolite (30–80 wt.%) and vitric or devitrified tuff with minor zeolite (0–10 wt.%). This variability in abundance combined with the geographic/depth heterogeneity suggests that smooth model distributions of zeolite (created by kriging) would not accurately capture the effect of zeolite on radionuclide transport. On the other hand, stochastic simulations of zeolite abundance based on the observed heterogeneities should provide a more realistic framework for investigating the amount of interaction between zeolite and radionuclides. In the next section, we describe the methodology for constructing zeolite distributions.

2.2. Generating zeolite distributions

The mineralogic model developed with Stratamodel interfaces to a compatible commercially available geostatistical software package (RC)². This interface allows geostatistical modeling to occur only with assigned stratigraphic units. The irregularly spaced mineralogic data and stratigraphic surfaces output from SGM are imported by (RC)² and then analyzed by constructing experimental horizontal and vertical variograms of mineral abundance. These variograms help define the spatial continuity through a quantitative description of how data values change as a function of distance and direction. Interpretive variogram models are then used in the process of performing ordinary kriging and sequential Gaussian simulations. Ordinary kriging provides a weighted linear estimate of values at unsampled areas and is generally a smoothing technique that results in a map of best fit values as well as a map of the uncertainty in the data (kriging variance). Sequential Gaussian simulations, on the other hand, produce conditional simulations that capture heterogeneity at finer scales than is possible with the smooth kriging map. Each simulation honors the data and always samples the same model variograms, but because the goal of the study was to examine the role of fine-scale heterogeneity, we used a sequential Gaussian simulation as the basis for subsequent flow and transport modeling.

Nevertheless, to analyze the results of the mineralogic modeling, we found it useful to construct both kriged and sequential simulations.

For simplicity, in this study, the horizontal variogram is chosen to be isotropic, so that the spatial correlation of zeolites in the east–west direction is assumed to be the same as the spatial correlation in the north–south direction. Using the available mineralogic data and stratigraphic model, $(RC)^2$ was used to calculate the experimental horizontal variogram along each stratigraphic layer, after which the software then fits a theoretical model to the experimental variogram. Fig. 1a shows the horizontal variogram chosen for the analyses. A vertical variogram was developed using a similar procedure and is shown in Fig. 1b. The horizontal variogram predicts a correlation length of 2000 m, whereas the vertical variogram suggests a correlation length of no more than 16 m. Because data are not sufficiently resolved to allow us to obtain the true vertical correlation length, the selection of 16 m is in part based on practical considerations. For example, despite the fineness of the numerical grid, there are limitations on how small a correlation length we can simulate. The node spacing within the portion of the grid where heterogeneous properties are mapped is on the order of 4 m. Therefore, choosing the maximum vertical correlation length suggested by the data (16 m) allows the simulation to capture vertical variability within several numerical grid cells. Regardless of the exact value for the vertical correlation length, there is a large difference in horizontal and vertical correlation lengths, and this is reflected in the simulation, resulting in thin (in the vertical) but very broadly distributed zones of zeolitization.

Fig. 2 shows the kriging estimate of the percent zeolitic abundance for both a north–south and an east–west cross-section. The estimate clearly shows the distinct zeolitic horizons that exist within the Calico Hill tuff. In general, kriging acts to smooth the data and therefore may not resemble the zeolitic distribution actually present in the field.

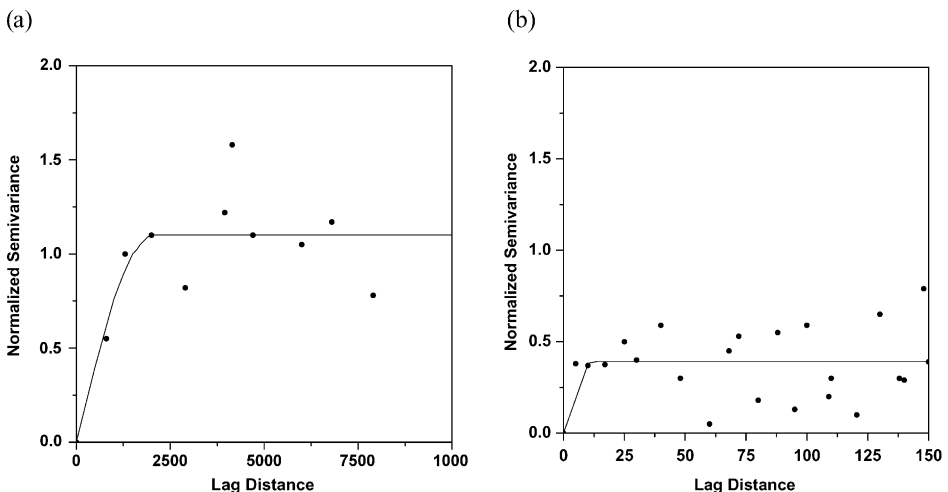


Fig. 1. Variograms depicting the spatial structure of the zeolites generated from $(RC)^2$ using data from the Calico Hills and Prow Pass units (a) horizontal variogram, (b) vertical variogram.

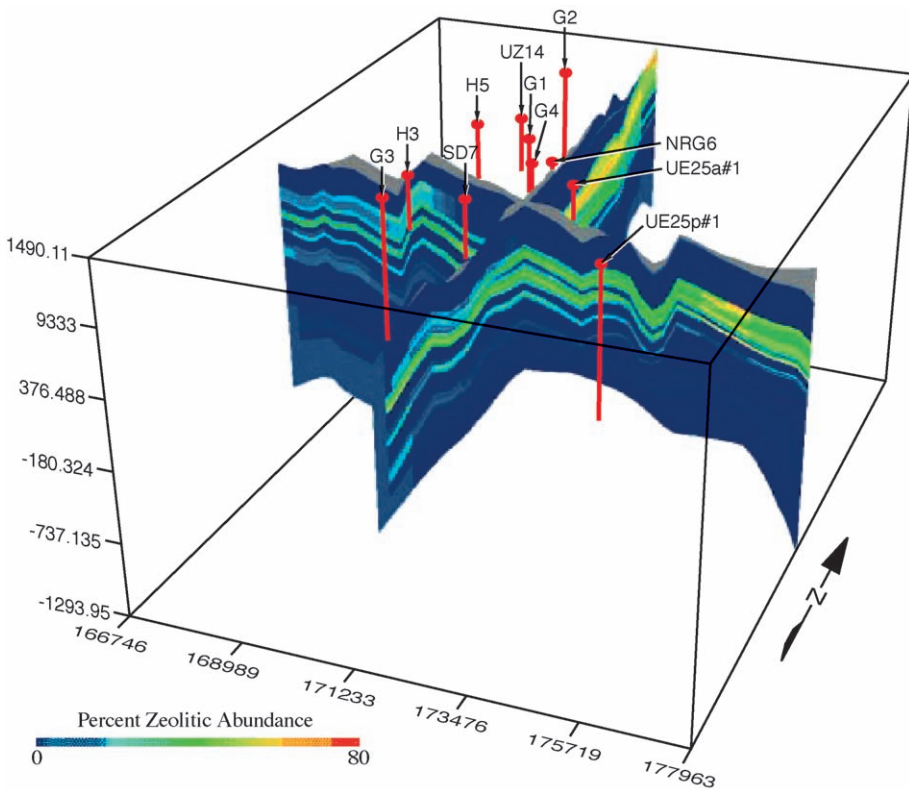


Fig. 2. Kriged zeolitic abundance of full mineralogical model.

To capture the small-scale variability using sequential Gaussian simulation yet maintain a model of manageable size, the mineralogical model domain was refined. For a heterogeneous mineralogical model useful for flow and transport simulations, the geostatistically simulated domain was constrained to lie between the Ghost Dance and Solitario Canyon faults, thereby capturing the variability within the potential repository block. With this smaller subset of the mineralogical model, a finer grid spacing (40 m) was chosen in the x and y directions, rather than the approximately 250 m of spacing of the full model, without greater computational expense. Because the horizontal variogram indicated that zeolitic abundance has a correlation length of about 2000 m, the 40 m of spacing in the x and y directions should be adequate to capture the small-scale heterogeneities in zeolitic abundance. The vertical direction already contained sufficient refinement and therefore remained the same as for the kriged model. Fig. 3 compares the kriged map to several conditional simulations. The kriged map clearly smooths out many of the small-scale heterogeneities that are present in the conditional simulations. Therefore, to investigate the influence of small-scale heterogeneity, the conditional simulations must be used to avoid eliminating potentially important variability from the model. Note also that the conditional simulations differ substantially at locations that are not close to well

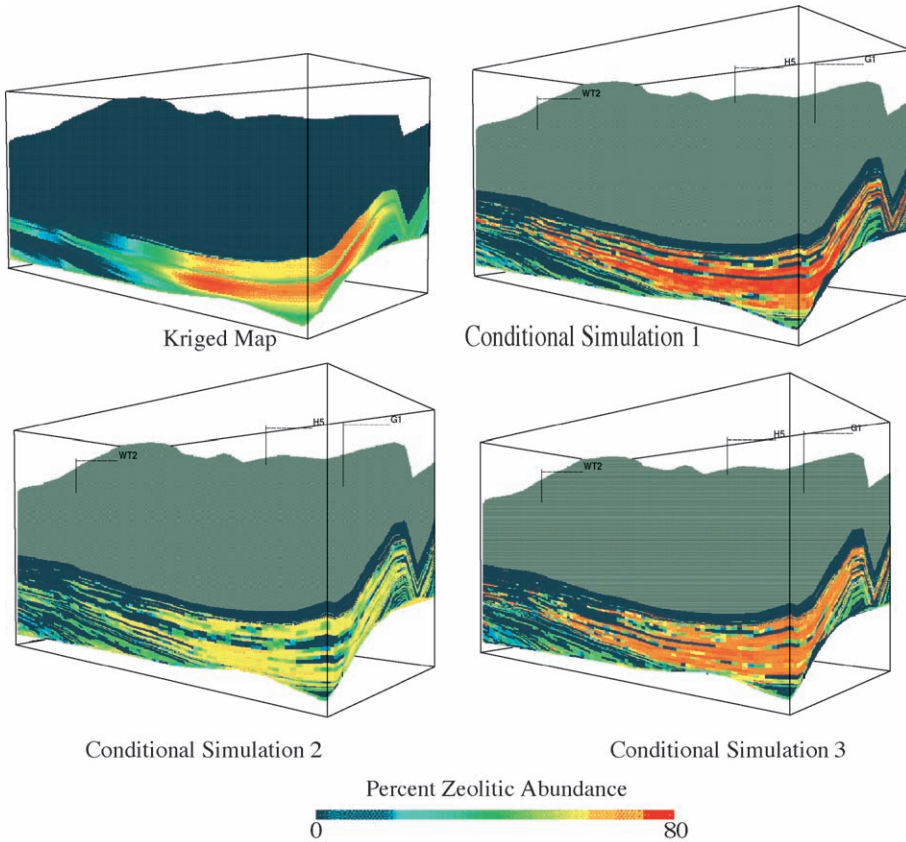


Fig. 3. Comparison of the kriged map and three conditional simulations.

locations, implying that if the purpose of the study was to evaluate the degree of uncertainty in travel times to the water table, it would be necessary to perform multiple realizations and compile statistical information on the results, such as mean and variance of the travel time. However, for this mechanistic study, a single realization should enable us to reveal important insights on the transport system.

3. Relationships between chemical and physical heterogeneity at Yucca Mountain

In this section, we examine various sources of laboratory and field data to determine whether the hydrologic parameters (permeability and characteristic curve parameters) and chemical parameters (distribution coefficient K_d) of the tuffs can be correlated to zeolitic abundance. Such correlations are expected because the physical and chemical properties of geologic medium can often be related back to fundamental measurable properties such as grain or pore size (Smith et al., 1996). Specifically, the process of zeolitic alteration acts to

reduce the pore sizes of the vitric tuffs. If such correlations could be developed, the zeolitic abundance can be used as the master variable, and its value can be used to compute the value of the secondary parameter at each location in the model domain.

The correlations presented are a combination of empirical relationships obtained from field data and theoretical relationships. Various researchers within the Yucca Mountain Project have developed several regression relationships. Theoretical relationships with physical bases also exist and could be used to correlate the various parameters. The following subsections describe relationships that are used to generate correlated parameters (permeability, characteristic curve parameters, and K_d).

3.1. Correlation between zeolitic abundance and permeability

Flint et al. (2001) developed a relationship between hydraulic conductivity (K_{sat}) and percent clinoptilolite for the Calico Hills tuff. The relationship is given by:

$$\log_{10}(K_{\text{sat}}) = -0.03845 \cdot \% \text{clinoptilolite} - 8.045 \quad r^2 = 0.47 \quad (1)$$

The data set is limited because data points exist at low and high values of zeolitic abundance, but are very sparse at intermediate values. The regression relationship clearly shows that there is not a 1:1 relationship between K_{sat} and the percent zeolite. However, zeolitic alteration clearly lowers the permeability of the tuff. Others have also shown that zeolitic alteration causes a large reduction in the hydraulic conductivity (e.g. Loeven, 1993), and numerical modeling studies of the Yucca Mountain unsaturated zone routinely use lower permeabilities for the zeolitic tuffs. Therefore, although the correlation coefficient of the regression is low, it captures a trend that is well established.

3.2. Correlation between zeolitic abundance and reactivity

Theoretical correlations between physical and geochemical heterogeneity for idealized porous media have been developed by Smith et al. (1996). Their derivation assumes that the permeability, porosity, and grain surface area are related through the concept of a hydraulic radius (Smith et al., 1996). The relationship is given by:

$$K_{d,m} = \frac{K_{d,a}}{\rho} \frac{\theta}{1-\theta} \sqrt{\frac{\theta}{2\tau k}} \quad (2)$$

where $K_{d,m}$ is the distribution coefficient based on the mass of rock, $K_{d,a}$ is the distribution coefficient based on surface area, ρ is grain density, τ is tortuosity, k is permeability, and θ is porosity. Eq. (2) shows that $K_{d,m}$ is inversely proportional to the square root of k for an ideal monomineralic porous media. It has not been determined whether this correlation is applicable to ^{237}Np migration through zeolitic tuff. Because the zeolitic abundance is the master variable in the present study, it is more straightforward to formulate a direct correlation between zeolitic abundance and K_d . To accomplish this, we examined sorption data for experiments performed by Triay et al. (1997). Triay et al. found that the K_d for ^{237}Np is a linear function of surface area, and furthermore that the preferential sorption

onto clinoptilolite can be explained by primarily using surface area arguments. Therefore, in the absence of direct data for reactivity as a function of either permeability or zeolite abundance, we propose that a simple linear relationship between zeolite abundance and K_d should be used, with $K_d=0$ for rock with no zeolite. In the numerical simulations, we vary the value of the slope of this correlation to reflect the uncertainty in K_d on zeolitic rocks established in these studies. We note in passing that although Eq. (2) is not used, use of the linear correlation between K_d and zeolite abundance and the K_{sat} relationship in Eq. (1) results in a trend toward higher sorption coefficient in less permeable rocks, albeit with a different mathematical relation than would be obtained using Eq. (2).

3.3. Correlation between permeability and characteristic curve parameters

The van Genuchten model (van Genuchten, 1980) was used for relating capillary pressure, fluid saturation, and permeability under unsaturated conditions. Qualitatively, the parameter α is inversely related to the air entry pressure, and the exponent n is inversely related to the width of the pore-size distribution. Therefore, a theoretical correlation between permeability and other characteristic curve parameters may be possible. Although no theoretical correlation has been found, an empirical relationship exists between α and permeability. Altman et al. (1996) performed a linear regression between the hydraulic conductivity (K_{sat}) and α using core data from the Calico Hills unit.

$$\log(\alpha) = -1.62 + 0.41\log(K_{sat}) \quad r^2 = 0.81 \quad (3)$$

where α is in units of 1/Pa and K_{sat} is in units of m/s. Since the range of n is only from 1.21 to 1.73, Altman et al. (1996) suggest that a constant mean value of 1.60 can be used. A constant residual saturation of 0.0453 is assumed for the Calico Hills tuffs. This parameter is obtained via fit to data rather than direct measurement, and is thus very poorly constrained. For this reason, we hold the value constant in the simulation.

3.4. Generating correlated parameters from maps of zeolitic abundance

With the correlations developed in the previous sections, the relevant properties can be distributed throughout the model domain. Ideally, the simulation process would allow us to generate, using zeolitic abundance as the master variable, realizations of multiple parameters (permeability, relative permeability, porosity, and K_d) which honor the univariate statistics of each parameter, the covariances between parameter, the spatial statistics of each parameter, and the spatial cross-covariances between parameter. With better data (more data points and tighter correlations between parameters), we could use co-simulation (Deutsch and Journel, 1992) or linear co-regionalization (Journel and Huijbregts, 1978; Luster, 1985) methods to distribute parameters. However, since the regression relationships have large error components and data are relatively sparse, we simply use the zeolitic abundance at each computational mesh point to compute K_{sat} (Eq. (1)) and K_d (linear relationship), and α is then determined from Eq. (3).

Using a direct 1:1 correlation could lead to unrealistic correlations which could overemphasize the possibility of a zeolitic bypass since zeolitic regions are assigned a

low permeability but high reactivity. However, the opposite case in which the hydrologic and chemical properties are uncorrelated can also lead to unrealistic transport results. We use the direct 1:1 correlations as an end member for transport behavior in the system in which hydrologic and chemical properties are correlated. The actual system behavior should fall in-between the uncorrelated case and the fully correlated case.

4. Flow and transport simulations

After each conditional simulation of zeolitic abundance is generated, the results are mapped onto the computational mesh. Conditional simulation 1 shown in Fig. 3 was mapped onto the refined Antler Ridge cross-section computational mesh and the result is shown in Fig. 4. Note that the conditional simulation is mapped between the Solitario Canyon and Ghost Dance faults. All zeolites outside this region simply contain the 10% zeolite cutoff since transport of ^{237}Np occurs primarily in the zeolites between the Solitario Canyon and Ghost Dance faults at this cross-section. Fig. 5 shows the zeolite distributions for the 10% and 20% cases. The 10% cutoff results in continuous layers of zeolites, whereas the 20% cutoff results in lenses of zeolites, illustrating the inherent problems with assigning an arbitrary cutoff value. We have chosen to simulate transport on the 10% cutoff case since this results in larger-scale zeolite distributions and serves as a better comparison to the small-scale zeolite variability in the conditional simulation. The contrasting scales of the two simulations make it possible to investigate the impact of small-scale variability of zeolites on radionuclide transport.

We utilize the finite element heat and mass transfer code (FEHM) (Zyvoloski et al., 1997) to study the hydrologic flow and ^{237}Np transport. FEHM is a three-dimensional heat and mass transport simulator that can represent complex structures (e.g. faults and stratigraphy) and model nonlinear processes such as vadose zone flow, heat flow, and

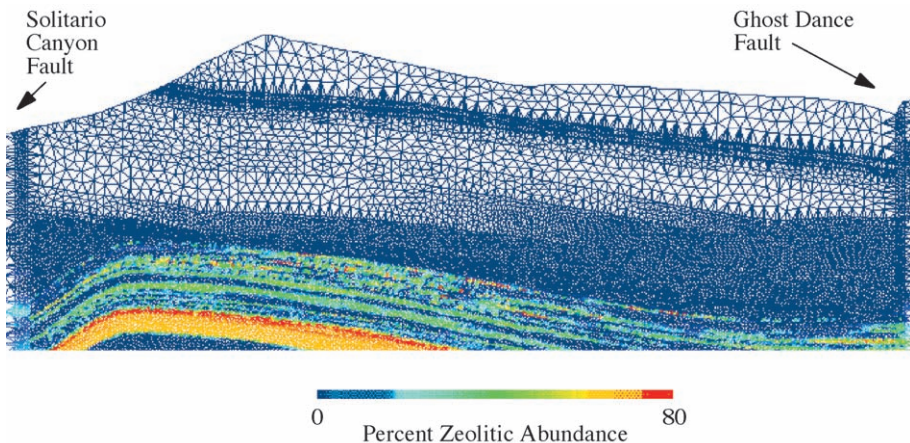


Fig. 4. Conditional simulation of percent zeolitic abundance mapped onto the computational mesh between the Solitario Canyon and Ghost Dance faults.

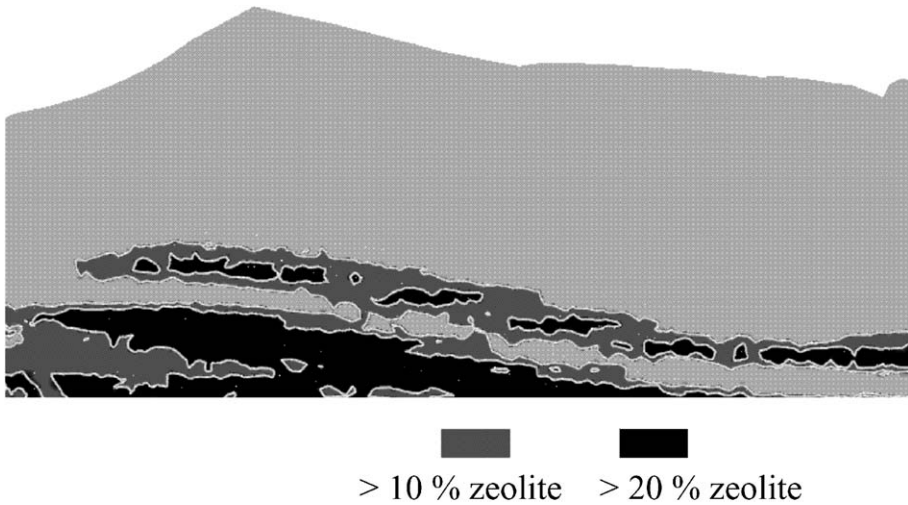


Fig. 5. Zeolitic distribution map for 10% and 20% cutoff cases.

multicomponent reactive transport. Detailed derivations of the governing equations for two-phase flow including heat have been described by several investigators (see, for example, Zyvoloski, 1983). In the unsaturated zone, the system of governing equations arises from the principles of conservation of water and air. Darcy's law is assumed to be valid for the movement of each phase. The relative permeability curves for the fracture and matrix continua are assumed to be represented by van Genuchten (1980). In simulations in the present study, the relative permeability curves for the fractured rock are assumed to be adequately represented by a dual permeability model (DKM). In this model formulation, fractures and matrix are treated as two overlapping continua, with appropriate properties assigned for each continuum. Additionally, there is a transfer term describing fluid flow between the two continua at each location in space. An additional parameter, a characteristic length scale for transport of heat, mass, and solutes between the two continua, is also required.

The assignment of parameter values for DKM that are appropriate for performing transport simulations is based on modeling work performed to calibrate the unsaturated zone flow model. The hydrologic parameters developed by Bodvarsson et al. (1999) were adopted with changes described below to represent the flow system. That modeling study presented calibration results assuming steady state flow conditions, using primarily measurements of matrix moisture content and matrix potential to achieve the fit. Parameters adjusted within the ranges of acceptable values include the fracture and matrix hydrologic parameters and the fracture–matrix connection area defined in the DKM formulation. All layers above the Calico Hills unit are assigned the property values of the parameter set reported in Appendix 6, Table 6.5.4-1 of Bodvarsson et al. (1999). This property set was derived by Bodvarsson et al. using a calibration to matrix fluid saturations assuming the base-case infiltration map of Flint et al. (2001). The Calico Hills and Prow Pass units are given permeabilities that correspond to zeolitic abundance. The relationship

between α and K_{sat} was used to assign values for α in the Calico Hills and Prow Pass units. Because insufficient information is available to correlate fracture properties to zeolite abundance or any other property, we assigned uniform fracture properties within these units, assuming values obtained by Bodvarsson et al. (1999) in their calibration study. For sorption, we use a simple linear relationship to relate K_d to zeolitic abundance. At 0% zeolite, we assume that no sorption of ^{237}Np will occur. We then choose different slopes to relate the zeolitic abundance to K_d . By running simulations at several different slopes, we bracket the variability in K_d .

Next, we describe the boundary conditions used to set-up the two-dimensional simulations of the Antler Ridge Cross Section. Flint et al. (2001) constructed estimated maps of temporally averaged infiltration rates based on models of surface soil hydrologic processes, calibrated with measurements of moisture content in shallow boreholes. Data from Flint et al. (2001) are used to simulate the infiltration rate with an infiltration varying between 0 and 20 mm/year in the modeled area with an average rate of 5 mm/year. The saturation along the bottom boundary is set to unity in order to simulate the water table. The left- and right-hand side boundaries are no flow boundaries. For consistency with the flow calibration modeling, the transport model results were obtained assuming steady state flow using the infiltration map of Flint et al. (2001) at this cross-section.

Fig. 6 shows the predicted matrix saturations for the conditional simulation, and the location of the well SD-12 projected onto this cross-section. Note that SD-12 is not exactly on the cross-section (it is 144 m north of the cross-section), so a direct comparison of model to data is not possible. The figure also shows field and model measurements of fluid saturation. The model measurements show good agreement with the field measurements. The saturation values reflect the variability in hydrologic properties in different stratigraphic units, and within the heterogeneous portion of the model, additional variability is introduced from the distributions of parameters used. In general, despite the heterogeneity, the saturation profiles look quite similar to the saturation profiles in simpler models that use a 10% threshold cutoff. However, this result should be considered in light of the fact that even small differences in fluid saturation could yield significant changes in flow paths and travel times through the medium. Also shown is the location of the potential repository where particles are released as a pulse injection at $t=0$ in the transport model. Fig. 7 compares the breakthrough curves at the water table (the distribution of residence times for a conservative solute) for the conditional simulation and a simplified 10% zeolite threshold model. As with the saturation distribution, the breakthrough curves look quite similar.

The differences in these two simulation approaches become apparent only when the retardation of ^{237}Np is included. This is shown in Fig. 8, which shows that for the conditional simulation, K_d has a large effect on the travel time. Each of the breakthrough curves represents a different slope of the linear K_d versus zeolite abundance relationship. Even for the low-sorption case in which K_d varies linearly with zeolitic abundance from 0 to 5 cm^3/g , the retardation is significant. Also shown in the figure is a simulation for the simplified 10% zeolite threshold model. Even a K_d of 20 cm^3/g within the zeolites does little to retard the transport through the unsaturated zone.

The process causing the larger retardation of ^{237}Np for the conditional simulation is a small, but significant, retardation due to sorption at locations with zeolite abundance less than 10%, rather than sorption within the high zeolite portions of the domain. Very little

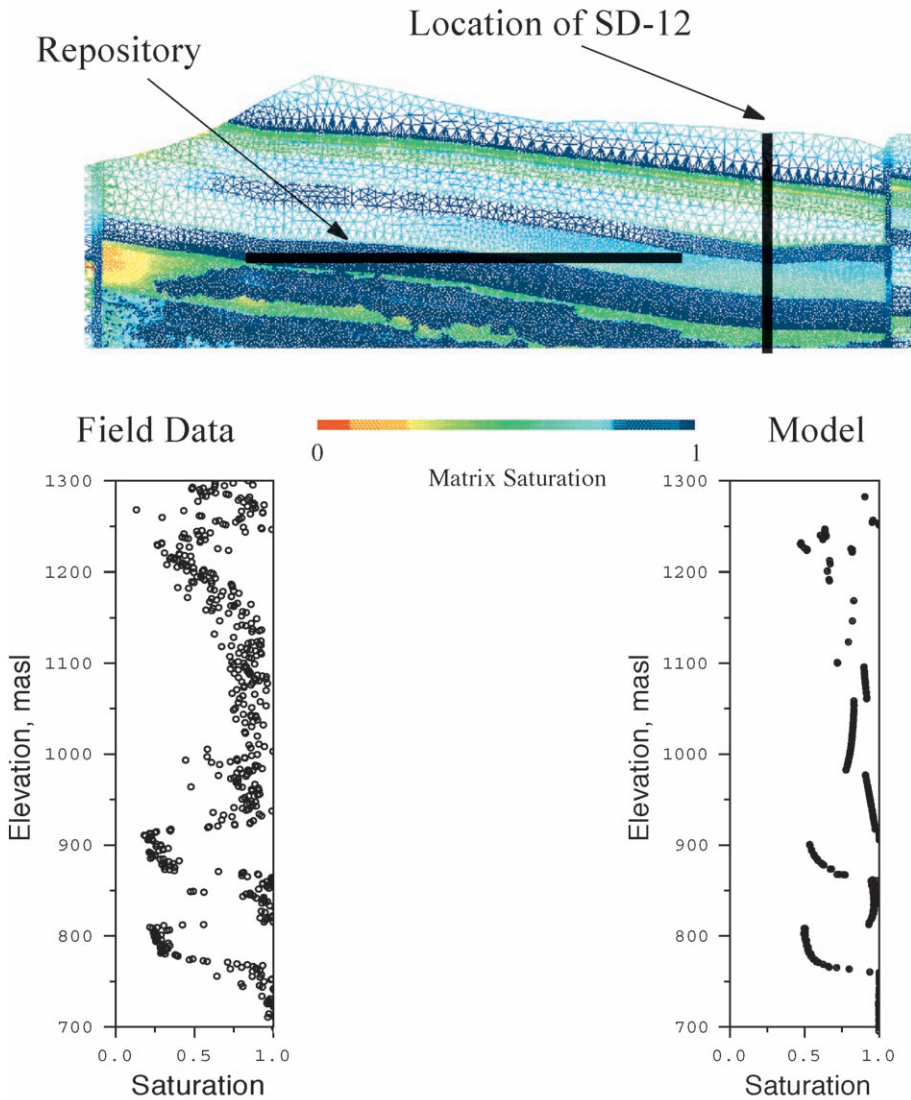


Fig. 6. Matrix saturation profile of the conditional simulation with comparison of model and simulations results for borehole SD-12.

flow travels through these highly zeolitized locations since they are very low in permeability. An extreme example of this fact is the 10% threshold case, for which a K_d of 20 cm³/g results in very little retardation. In the dual permeability model used, transport through fractures in the zeolites provides a bypass mechanism, and the radionuclide has little access to the sorptive rock. An alternate conceptual model of sparse or impermeable fractures in the zeolites would probably yield large-scale bypassing around

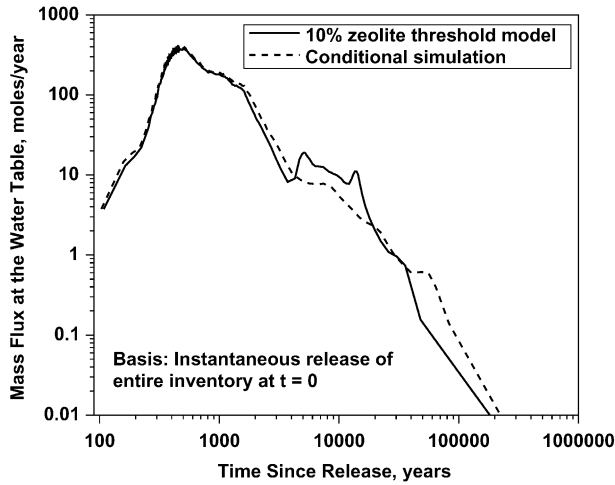


Fig. 7. Comparison of the 10% threshold method and the conditional simulation.

the zeolitic rock. However, from the standpoint of retardation due to sorption on the zeolites, the results would be the same.

This result calls into question the validity of the simplified model approach employing a threshold percentage because of the dramatically different travel time distributions obtained. A workable solution to this problem can be obtained by recognizing that retardation in the heterogeneous model is not due to the regions of high zeolite abundance

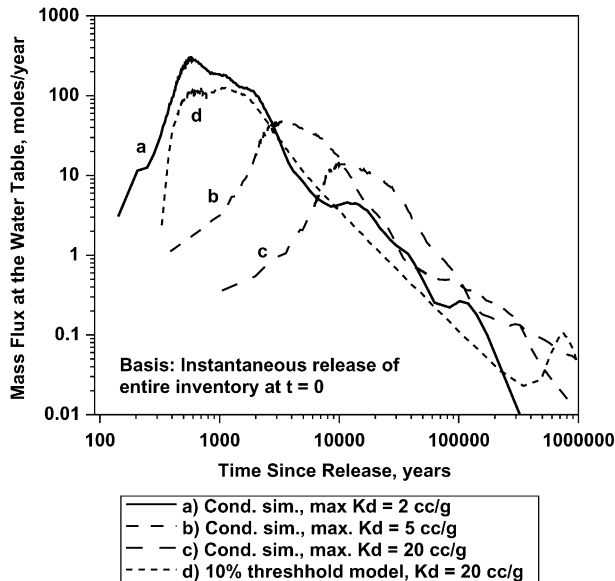


Fig. 8. Comparison of conditional simulation using different K_d s and the 10% threshold model.

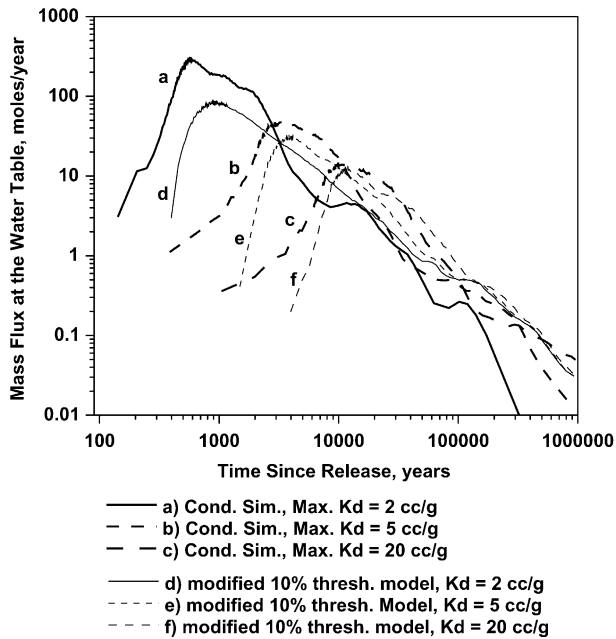


Fig. 9. Modification of the 10% threshold method to better match the conditional simulation. The dotted lines show the results when all rocks with zeolitic abundance less than 10% are assigned a K_d of $0.1K_d$.

but by the more permeable rocks with high enough permeability to transmit fluids through the rock matrix. This suggests that in the simplified models, assigning a small K_d (just 10% of the maximum K_d) to all locations with zeolite abundance between 0% and 10% would yield behavior more similar to the heterogeneous cases. In the 10% threshold case, this would be in the portions of the Calico Hills tuffs that are assigned vitric tuff properties. Fig. 9 shows that modifying the 10% threshold case in this manner more closely matches the conditional simulation. Although this analysis has been performed for only one conditional simulation, similar results should be obtained regardless of the precise distribution of zeolite abundance because the water containing the radionuclides will preferentially travel through the more permeable portions of the unsaturated zone.

5. Discussion and conclusions

Small-scale variability of chemical and hydrologic properties can play an important role on the prediction of flow and transport in the unsaturated zone. The variation in chemical and hydrologic properties is strongly dependent on the mineral distribution. Due to the correlation between mineral distribution and hydrologic and chemical properties, the distribution of minerals such as zeolites can strongly influence the flow patterns of percolating fluids and the sorption of many radionuclides. In this manuscript, the zeolitic threshold method used in previous studies is compared to a more rigorous geostatistical

modeling. With this more sophisticated modeling approach, we examine whether using a threshold cutoff for zeolitic abundance is an appropriate upscaling method for incorporating the effects of small-scale heterogeneity.

A key conclusion from the comparison is that the retardation due to sorption predicted by a conditional simulation is much larger than the retardation predicted by the zeolite threshold method. The reason for larger retardation of ^{237}Np for the conditional simulation is a small but significant K_d at locations with zeolite abundance less than 10%. At these locations, the K_d is low (less than $1 \text{ cm}^3/\text{g}$) but permeability is large enough for the flow to be matrix dominated. Most models to date have treated the zeolitic Calico Hills unit as thick and continuous units of very low matrix permeability, requiring flow to either bypass the sorptive minerals via fracture flow or to travel laterally around the zeolites. The geostatistical model, which we believe to be more realistic, results in bypassing only the regions with the highest zeolite abundances, as those rocks with lower zeolitic content possess higher matrix permeability in the model. This result is somewhat tentative due to the uncertain nature of several of the correlations applied to populate the model. The inverse correlation between permeability and zeolite content, though clearly correct at the two ends of high and low zeolite abundance, is based on sparse data at intermediate values. Therefore, we recommend that future core sampling and hydrologic property measurements focus on this intermediate range. This conclusion also applies to sorption data. In fact, measurements of all the properties of interest on the same rock samples are the best way to tighten the correlations used.

The geostatistical model result calls into question the validity of the simplified model approach employing a cutoff percentage. More bypassing of the zeolites occurs in models in which large and continuous regions of low-permeability rock are present in the model. To correct this deficiency in simplified models, we demonstrated that modifying the 10% threshold case to include some sorption at locations with zeolite abundances less than 10% results in closer agreement to the more rigorous conditional simulation. For the purposes of abstracting these results, setting nonzero K_d s in the vitric tuffs may be an effective way to mimic the more rigorous conditional simulation. We note that the Total Systems Performance Assessment (TSPA) models have taken this approach, assigning K_d values in the vitric tuff for ^{237}Np that are smaller than the K_d in the zeolitic tuffs, but nevertheless greater than zero (DOE, 1998).

Another drawback of the simplified approach is that there may be introduced large-scale flow patterns within the unsaturated zone that do not occur when smaller-scale heterogeneity is considered. For example, if the cutoff extends as low as 10%, large volumes of rock will probably be assigned permeability values that are smaller than they actually are. In the absence of fracturing, large-scale lateral diversion will result in the model. It is likely that a heterogeneous rock mass would impede downward migration, perhaps even causing perched water, but without resulting in an impermeable barrier. Such a model would yield substantially better performance of the UZ barrier than one in which water is diverted laterally to the water table or to a fault. Because in large-scale models, it is computationally expensive to populate the domain with heterogeneous properties, a useful alternative might be to subdivide the zeolitic Calico Hills tuff into a small number of zones of equal zeolite abundance, and assign property values consistent with the correlations developed in this study.

We note that one limitation of the present study is that we present results from a single conditional simulation. In order to draw more substantial conclusions, such as the uncertainty in travel times given our current state of knowledge, many more conditional simulations would need to be performed. Nevertheless, we believe that similar results should be obtained regardless of the precise distribution of zeolite abundance because in all cases, the water containing the radionuclides will preferentially travel through the more permeable portions of the unsaturated zone. With respect to the methodology and data availability, as mentioned earlier, better laboratory data are needed to refine the correlations and variograms and implement linear co-regionalization models. Such models build the scatter in the correlations directly into the distribution of parameter values in a rigorous way. In addition, potential correlations between fracture permeability and zeolitic abundance should be investigated to extend the model. Such information would need to be collected at the field scale. Finally, the data available to construct the variograms are exclusively from analyses of borehole samples. Though this represents a good start, the characterization of the Calico Hills tuff would be vastly improved with a drift constructed into this rock beneath the potential repository. A more complete picture of the distribution of minerals, hydrologic properties, and fracturing would emerge from such a characterization effort. In addition, rocks that likely provide a barrier to radionuclide migration would be accessible for direct-field testing. In conclusion, this study presents a general framework for integrating geostatistical information into the site-scale flow and transport calculations. These powerful tools provide a means for determining the uncertainties associated with radionuclide transport through the unsaturated zone at scales not normally studied in site-scale models. We believe that such models, which more rigorously incorporate the available data into the simulations, can augment simpler site-scale models by assessing the validity of simplifying assumptions and providing guidance on how to allow simpler models to mimic the flow and transport behavior of a more realistic representation of the distribution of rock properties.

Acknowledgements

This work was supported by the Yucca Mountain Site Characterization Office as part of the Civilian Radioactive Waste Management Program, which is managed by the US Department of Energy, Yucca Mountain Site Characterization Project. The authors thank the two reviewers of this manuscript for their excellent review comments and suggestions.

References

- Altman, S.J., Arnold, B.W., Ho, C.K., McKenna, S.A., Barnard, R.W., Barr, G.E., Eaton, R.E., 1996. Flow calculations for Yucca Mountain ground water travel time (GWTT-95). Technical Report SAND96-0819, Sandia National Laboratories.
- Andrews, R.W., et al., 1995. Total System Performance Assessment—1995, An Evaluation of the Potential Yucca Mountain Repository, TRW Document number B00000000-01717-2200-00136, Rev. 01, November.
- Birkholzer, J., Tsang, C.F., 1997. Solute channeling in unsaturated heterogeneous porous media. *Water Resour. Res.* 33 (10), 2221.

- Bodvarsson, G.S., Boyle, W., Patterson, R., Williams, D., 1999. Overview of scientific investigations at Yucca Mountain—the potential repository for high-level nuclear waste. *J. Contam. Hydrol.* 1–3 (38), 3–24.
- Carey, J.W., Chipera, S.J., Vaniman, D.T., Bish, D.L., Viswanathan, H.S., Carter-Krogh, K., 1997. Three-Dimensional Mineralogic Model of Yucca Mountain, Nevada. LANL Milestone Report Deliverable No. SP344BM4, September 30, 1997. Los Alamos National Laboratory, Los Alamos, NM. RIS Accession # MOL.19971117.0110.
- Chipera, S.J., Bish, D.L., 1995. Multireflection RIR and intensity normalizations for quantitative analyses: applications to feldspars and zeolites. *Powder Diffr.* 10 (1), 47–55.
- Deutsch, C.V., Journel, A.G., 1992. *GSLIB: Geostatistical Software Library and User's Guide*. Oxford University, New York, p. 340.
- DOE (US Department of Energy), 1998. Overview—Viability Assessment of a Repository at Yucca Mountain. DOE/RW-0508. Washington, DC: US Department of Energy, Office of Civilian Radioactive Waste Management.
- Flint, A.L., Flint, L.E., Bodvarsson, G.S., Kwicklis, E.M., Fabryka-Martin, J., 2001. Evolution of the conceptual model of unsaturated zone hydrology at Yucca Mountain, Nevada. *J. Hydrol.* 1–2 (247), 1–30.
- Gelhar, L.W., 1993. *Stochastic Subsurface Hydrology*. Prentice-Hall, Englewood Cliffs, NJ.
- Journel, A.G., Huijbregts, Ch.J., 1978. *Mining Geostatistics*. Academic Press, New York, p. 600.
- Landmark Graphics, 1995.
- Loeven, C., 1993. A summary and discussion of hydrologic data from the Calico Hills nonwelded hydrogeologic unit at Yucca Mountain, Nevada. Technical Report LA-12376-MS, Los Alamos National Laboratory.
- Luster, G.R., 1985. Raw Materials for Portland Cement: Applications of conditional simulation of coregionalization. PhD dissertation, Stanford, CA: Stanford University, Department of Applied Earth Sciences, p. 531.
- Robinson, B.A., Wolfsberg, A.V., Viswanathan, H.S., Bussod, G.Y., Gable, C.W., Meijer, A., 1997. The Site-Scale Unsaturated Zone Transport Model of Yucca Mountain. Yucca Mountain Site Characterization Project Milestone SP25BM3.
- Smith, R.W., Schafer, A.L., Tompson, A.F.B., 1996. Theoretical relationships between reactivity and permeability for monomineralic porous media. In: Murphy, W.M., Knecht, D.F. (Eds.), *Proceedings XIX Symposium of the Scientific Basis for Nuclear Waste Management*. Mater. Res. Symp. Proc., vol. 412, pp. 693–700.
- Tompson, A.F.B., Jackson, K.J., 1996. Reactive transport in heterogeneous systems. *Rev. Miner.* 34 (1), 269–308.
- Tompson, A.F.B., Schafer, A.L., Smith, R.W., 1996. Impacts of physical and chemical heterogeneity on cocontaminant transport in sandy porous medium. *Water Resour. Res.* 26 (10), 2541–2562.
- Triay, I.R., et al., 1997. Summary report geochemistry/transport laboratory tests. Los Alamos National Laboratory, YMP Milestone SP23QM3 (Something better Bruce?).
- van Genuchten, M.T., 1980. A closed form equation for predicting hydraulic conductivity of unsaturated soils. *Soil Sci. Soc. Am. J.* 44, 892–898.
- Zelinski, W.P., Clayton, W.R., 1996. A 3-D geologic framework and integrated site model of Yucca Mountain: Version ISM 2.0.
- Zyvoloski, G.A., 1983. Finite element methods for geothermal reservoir simulations. *Int. J. Numer. Anal. Methods Geomech.* 7, 75–86.
- Zyvoloski, G.A., Robinson, B.A., Dash, Z.V., Trease, L.L., 1997. Summary of the models and methods for the FEHM application—a finite-element heat- and mass-transfer code. Los Alamos National Laboratory Report LA-13307-MS.